Supramolecular Chemistry
Publication details, including instructions for authors and subscription information:
http://www.informaworld.com/smpp/title~content=t713649759

Potentiometric Titrations and Nickel(II) Complexes of Four Topologically Constrained Tetraazamacrocycles

Timothy J. Hubin[a]; Nathaniel W. Alcock[b]; Howard J. Clase[b]; Daryle H. Busch
[a] Department of Chemistry, The University of Kansas, Lawrence, KS, USA [b] Department of Chemistry, The University of Warwick, Coventry, England

To cite this Article Hubin, Timothy J. , Alcock, Nathaniel W. , Clase, Howard J. and Busch, Daryle H.(2001) 'Potentiometric Titrations and Nickel(II) Complexes of Four Topologically Constrained Tetraazamacrocycles', Supramolecular Chemistry, 13: 2, 261 — 276
To link to this Article: DOI: 10.1080/10610270108027481
URL: http://dx.doi.org/10.1080/10610270108027481

SUPRAMOLECULAR CHEMISTRY, Vol. 13, pp. 261–276
Reprints available directly from the publisher
Photocopying permitted by license only

Potentiometric Titrations and Nickel(II) Complexes of Four Topologically Constrained Tetraazamacrocycles

TIMOTHY J. HUBIN[a], NATHANIEL W. ALCOCK[b], HOWARD J. CLASE[b] and DARYLE H. BUSCH[a,*]

[a]*Department of Chemistry, The University of Kansas, Lawrence, KS 66045, USA;* [b]*Department of Chemistry, The University of Warwick, Coventry CV4 7AL, England*

(Received 26 July 2000)

The novel high spin Ni^{2+} complexes of the topologically constrained tetraazamacrocycles (1–4) [4,11-dimethyl-1,4,8,11-tetraazabicyclo[6.6.2]hexadecane (1); 4,10-dimethyl-1,4,7,10-tetraazabicyclo[6.5.2]pentadecane (2); 4,10-dimethyl-1,4,7,10-tetraazabicyclo[5.5.2]tetradecane (3); *racemic*-4,5,7,7,11,12,14,14-octamethyl-1,4,8,11-tetraazabicyclo[6.6.2]hexadecane (4)] show striking properties. Potentiometric titrations of the ligands 2 and 4 revealed them to be proton sponges, as reported earlier for 1 [1]. Ligand 3 is less basic, losing its last proton with a pK = 11.3(2). Despite high proton affinities, complexation reactions in the absence of protons successfully yielded Ni^{2+} complexes in all cases. The X-ray crystal structures of $Ni(1)(acac)^+$, $Ni(3)(acac)^+$ and $Ni(1)(OH_2)_2^{2+}$ demonstrate that the ligands enforce a distorted octahedral geometry on Ni^{2+} with two *cis* sites occupied by other ligands. Magnetic measurements and electronic spectroscopy on the corresponding $Ni(L)Cl_2$ (L = 1–3) complexes reveal that all are high spin and six-coordinate with typical magnetic moments. In contrast, $[Ni(4)Cl^+]$ is five-coordinate with a slightly higher magnetic moment and its own characteristic electronic spectrum. The extra methyl groups on ligand 4 define a shallow cavity, sterically allowing only one chloride ligand to bind to the nickel(II) ion.

Keywords: Bridged macrocycles; Macrocyclic nickel complexes; Topologically constrained ligands; Tetraazamacrocycles; Proton sponges; Potentiometric titrations; Ligand basicities

INTRODUCTION

The principles of modern coordination chemistry [2] should allow us to design ligands that would be strikingly resistant to oxidative hydrolysis while still having available sites for direct binding of the metal ion to small molecules, perhaps oxidants or substrates in catalytic systems. The importance of having two *cis* labile sites (as in the complexes of **1** and **2**) has been discussed in relation to various catalytic and biomimetic processes [3]. The obvious ligand to satisfy these relationships is 1,4,7,10-tetraazacyclododecane, often labeled *cyclen*, or, systematically, [12]aneN4. It binds to first row transition ions exclusively in a folded conformation

*Corresponding author. e-mail: dbusch@caco3.chem.ukans.edu

because its internal cavity is too small to encompass those metal ions. With the tetraazamacrocyclic ligand in such a conformation, the remaining two metal ion sites are, of course, adjacent to each other (*cis*). The principal limitation of cyclen in such catalytic roles arises because of its folded conformation. It has frequently been demonstrated with other macrocyclic complexes that folded systems release metal ions much more rapidly than do planar macrocycles [4]. These and other considerations led to our study of the ligands used in the studies reported here.

For a given donor atom set, both the thermodynamic and kinetic stabilities of metal complexes generally increase in the series *monodentate ligand < linear or branched chelating ligand < macrocyclic ligand < macrobicyclic ligand, or cryptate*. This sequence may be rationalised as: complex stability increases with the topological complexity of the ligand, given equal complementarity [2]. Thus, to retain the features that cyclen would produce in an octahedral complex while achieving a level of stability comparable to the strongest complexes, a tetradentate ligand is required that is as topologically constrained as the macrobicyclic cryptates. This led us to examine cross-bridged tetraazamacrocycles (Fig. 1, Structures **1–4**) [5–8], some of which have already been recorded before our studies began; however, they had not been fully exploited as transition metal ligands. Their proton-sponge nature has been quantified by the potentiometric titration data given below. They present a great challenge to the synthesis of complexes with all but the strongest binding transition metal ions [6, 9]. Our recent work has overcome this problem to produce a wide range of transition metal complexes [10], including those of the biologically relevant Cu(II), Mn(II) and Fe(II) [1, 8].

To broaden the range of metal complexes of these ligands, we report here the synthesis of the Ni^{2+} complexes with the topologically constrained ligands **1–4**, the chemical and physical

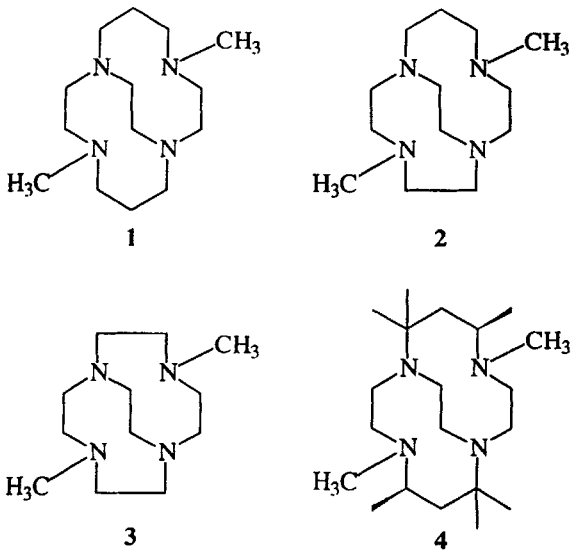

FIGURE 1 Chemical structures of ligands 4,11-dimethyl-1,4,8,11-tetraazabicyclo[6.6.2]hexadecane **1**(a) [5, 6]; 4,10-dimethyl-1,4,7,10-tetraazabicyclo[6.5.2]pentadecane 2(b) [6, 7]; 4,10-dimethyl-1,4,7,10-tetraazabicyclo[5.5.2]tetradecane 3(c) [6]; and *racemic*-4,5,7,7,11,12,14,14-octamethyl-1,4,8,11-tetraazabicyclo[6.6.2]hexadecane **4**(d) [8].

properties of the new complexes, and the X-ray crystal structures of two of them. Nickel(II) has historically been much studied in its complexes with tetraazamacrocycles due to its ease in handling (lack of oxygen sensitivity), useful spectroscopic properties, and preference for square planar coordination geometry which matches the arrangement of donors in typical tetraazamacrocycles. For similar reasons, nickel(II) has often been exploited in template syntheses of tetraazamacrocycles [4b, 11]. Nickel(II), therefore, provides a basis for comparison of these new ligand systems with examples from classical coordination chemistry.

EXPERIMENTAL SECTION

$Ni(acac)_2$ (95%), $NiCl_2$ (99.99%), NH_4PF_6 (95%) were purchased from Aldrich Chemical Company and were used as received. [13]aneN4 was purchased from the Kansas Advanced Synthetic Laboratory of the University of Kansas. All

solvents were of reagent grade and were dried, when necessary, by accepted procedures [12].

Elemental analyses were performed by the Analytical Service of the University of Kansas, Desert Analytics, or Quantitative Technologies, Inc. Mass spectra were measured by the Analytical Service of the University of Kansas on a VG ZAB HS spectrometer equipped with a xenon gun. The matrix used was NBA (nitrobenzyl alcohol).

Synthesis

4,11-Dimethyl-1,4,8,11-tetraazabicyclo[6.6.2]hexadecane, (**1**), 4,10-dimethyl-1,4,7,10-tetraazabicyclo[6.5.2]pentadecane (**2**) and 4,10-dimethyl-1,4,7,10-tetraazabicyclo[5.5.2]tetradecane (**3**), were synthesized according to literature procedures [5, 6]. A full description of the synthesis of *racemic*-4,5,7,7,11,12,14,14-octamethyl-1,4,8,11-tetraazabicyclo[6.6.2]hexadecane (**4**) can be found elsewhere, including structural characterization of various precursors [8].

4,10-Dimethyl-1,4,7,10-tetraazabicyclo[6.5.2]pentadecane tris(hydrochloride)monohydrate (2·3HCl·H_2O)

To 400 mg (2.00 mmol) of (**2**) dissolved in 5 ml of dry ethanol was added 5 ml of concentrated hydrochloric acid, dropwise at first and then in larger portions. After the addition was complete, the reaction was stirred for ~15 min., during which time the initial white precipitate redissolved. The ethanol, water and excess HCl were removed under vacuum to give a waxy white solid, which was taken up in 30 ml of dry methanol. Diethyl ether (300 ml) was added and the mixture chilled at 0°C for 1 h. The white precipitate was recovered by filtration, washed copiously with dry ether, and partially dried on the frit. Further drying of the solid was accomplished in vacuo. The crude ligand salt was recrystallized from dry methanol by addition of dry ether to the onset of turbidity, followed by cooling in a freezer. Filtration of the resulting solid, washing with dry ether and drying gave 600 mg (98%) of the white solid product. Anal. calc. for $C_{13}H_{33}N_4O_4Cl_3$: C 42.45%, H 9.04%, N 15.23%; found: C 42.39%, H 9.19%, N 14.88%.

4,11-Dimethyl-1,4,7,10-tetraazabicyclo[5.5.2]tetradecane tris(hydrochloride)dihydrate (3·3HCl·2H_2O)

To 1.36 g (6 mmol) of (**3**) dissolved in 15 ml of dry ethanol was added 5 ml of concentrated hydrochloric acid, dropwise at first and then in larger portions. After the addition was complete, the white precipitate was removed by filtration and washed with ethanol, then ether. The crude ligand salt was recrystallized from dry methanol by addition of dry ether to the onset of turbidity, followed by cooling in a freezer. Filtration of the resulting solid, washing with dry ether and drying gave 1.80 g (81%) of the off-white solid product. Anal. calc. for $C_{12}H_{33}N_4Cl_3O_2$: C 38.77%, H 8.61%, N 15.07%; found: C 39.13%, H 8.76%, N 15.04%.

Racemic-4,5,7,7,11,12,14,14-octamethyl-1,4,8,11-tetraazabicyclo[6.6.2]hexadecane bis(trifluoroacetate)hydrate (4·2TFA·H_2O)

To 500 mg (1.5 mmol) of (**4**) dissolved in 20 ml of dry methanol was added 5 eq (855 mg) of trifluoroacetic acid (TFA) dropwise. After the addition was complete, the solvent and excess TFA were removed under vacuum to give an oil which solidified upon addition of ether and cooling at 0°C. The crude ligand salt was collected by filtration and recrystallized three times from dry acetonitrile by addition of dry ether to the onset of turbidity, followed by cooling in a freezer. Filtration, washing with dry ether and drying gave 570 mg (65%) of the off-white solid product. Anal. calc. for $C_{24}H_{46}N_4O_5F_6$: C 49.31%, H 7.93%, N 9.58%; found: C 49.52%, H 7.77%, N 9.67%.

[NiL(acac)][Ni(acac)$_3$]·THF(L = 1, 3)

The ligand (1 mmol) was dissolved in 5 ml of dry THF in a 25 ml Erlenmeyer flask under an inert atmosphere. A solution of 257 mg (1 mmol) of Ni(acac)$_2$ in 5 ml of dry THF was added dropwise to the stirring ligand solution. The reaction was stirred for 16 h, then filtered to remove trace amounts of a gray-white solid from the golden filtrate. Ether diffusion into the THF solution yielded large pale purple hygroscopic crystals suitable for X-ray diffraction. Yield: 30–43% based on ligand.

[Ni(1)(acac)][Ni(acac)$_3$]·THF

Anal. Calc. for $C_{38}H_{66}N_4Ni_2O_9$: C 54.31%, H 7.92%, N 6.67%; found: C 54.00%, H 8.10%, N 6.58%.

[Ni(3)(acac)][Ni(acac)$_3$]·THF

Anal. Calc. for $C_{36}H_{62}N_4Ni_2O_9$: C 53.23%, H 7.69%, N 6.90%; found: C 52.93%, H 7.50%, N 6.80%. FAB$^+$ mass spectra in THF (L = **1**) or MeOH (L = **3**) (NBA matrix) exhibited peaks at m/z = NiL(acac)$^+$ for both complexes.

NiLCl$_2$(L = 1–3) and [Ni(4)Cl]PF$_6$

The ligand (1 mmol) was dissolved in 20 ml of dry DMF in a 25 ml Erlenmeyer flask in an inert atmosphere glovebox. Anhydrous $NiCl_2$ (130 mg, 1 mmol) was added to the stirring ligand solution. The reaction mixture was stirred for 16 h at 50–60°C, giving blue to blue-green solutions when all of the $NiCl_2$ dissolved (after about 2 h). The cooled solution was removed from the glovebox, where addition of 400 ml of ether resulted in a powdered product. Filtration, followed by washing with 100 ml of ether and drying in vacuo gave the hygroscopic products for L = **1**–**3**. For [Ni(**4**)Cl]PF$_6$, the chloride salt was found to be insufficiently pure, so it was dissolved in a minimum amount of dry MeOH and excess NH_4PF_6 was added. The solution was stirred and cooled to 0°C until precipitation of the product was complete. The green product was collected by filtration, washed with MeOH and ether and dried in vacuo. Yields: 69–89% based on the ligand. **Ni(1)Cl$_2$·2H$_2$O**. Anal. Calc. for $C_{14}H_{34}N_4NiCl_2O_2$: C 40.03%, H 8.16%, N 13.34%; found: C 39.69%, H 7.80%, N 13.42%. **Ni(2)Cl$_2$@H$_2$O**. Anal. Calc. for $C_{13}H_{30}N_4NiCl_2O$: C 40.24%, H 7.79%, N 14.44%; found: C 40.39%, H 7.67%, N 14.43%. **Ni(3)Cl$_2$·0.5H$_2$O**. Anal. Calc. for $C_{12}H_{27}N_4NiCl_2O_{0.5}$: C 39.49%, H 7.46%, N 15.35%; found: C 39.71%, H 7.46%, N 15.73%. **[Ni(4)Cl]PF$_6$**. Anal. Calc. for $C_{20}H_{42}N_4NiClPF_6$: C 41.58%, H 7.33%, N 9.70%; found: C 41.22%, H 7.06%, N 9.41%. FAB$^+$ mass spectra in H_2O (L = **1**), DMF (L = **2**, **3**), or MeCN (L = **4**) (NBA matrix) exhibited peaks at m/z = NiLCl$^+$ for all complexes. Crystals of the L = **1** complex were obtained by ether diffusion into an acetonitrile solution of the complex.

Physical Methods

Electrochemical experiments were performed on a Princeton Applied Research Model 175 programmer and Model 173 potentiostat in dry CH_3CN using a homemade cell in an inert atmosphere dry box under N_2. A button Pt electrode was used as the working electrode in conjunction with a Pt-wire counter electrode and a Ag-wire pseudo-reference electrode. Tetrabutylammonium hexafluorophosphate (0.1 M) was the supporting electrolyte in all cases. The measured potentials were referenced to SHE using ferrocene (+0.400 V *versus* SHE) as an internal standard.

Magnetic studies were performed in the solid state on a Johnson Matthey MSBI magnetic suscebtibility balance. Diamagnetic corrections were based on literature values [13]. Conductance measurements [14] were obtained with a YSI Model 35 conductance meter at room temperature on 1 mM solutions. Potentiometric titrations were performed under N_2 at 25.0°C

with an ionic strength of 0.1000 (KNO_3) on a Brinkmann Metrohm 736GP Titrino equipped with a Brinkmann combination electrode. The electrode was standardized by a three buffer calibration using the Titrino's internal standardization method, followed by titration of a standardized strong acid (HNO_3) with a standardized strong base (KOH) after a literature procedure [15]. The strong acid and the strong base solutions were prepared from carbonate-free water and standardized by Titrino's internal methods. The KOH solution was stored under N_2 to minimize carbonate formation. In a typical titration $\sim$10 mg of the material to be titrated was placed in 50.0 ml of the supporting electrolyte solution and $\sim$2 ml of the HNO_3 solution was added to a $p[H^+] < \sim 3$. The resulting solution was titrated to a $p[H^+]$ value between 11 and 12. The data were fit using the program BETA [16], which is an updated version of a previous program of the same name [17], using the pK_w found in the strong acid/base titration. For (**2**), 4 replicate titrations were performed each with a goodness of fit $(GOF)^{15} < 2.4$ and a total of 2404 data points. For (**3**) 4 replicate titrations were performed each with a goodness of fit $(GOF)^{15} < 2.3$ and a total of 2404 data points. For (**4**) 4 replicate titrations were performed each with a goodness of fit $(GOF)^{15} < 1.8$ and a total of 1701 data points.

Crystal Structure Analysis

X-ray data were collected with a Siemens SMART [18] three-circle system with CCD area detector using graphite monochromated Mo-Kα radiation ($\lambda = 0.71073$ Å). The crystals were held at the specified temperature with the Oxford Cryosystem Cooler [19]. Absorption corrections were applied by the Ψ-scan method, and none of the crystals showed any decay during data collection.

The structures were solved by direct methods using SHELXS [20] (TREF) with additional light atoms found by Fourier methods. Hydrogen atoms were added at calculated positions and refined using a riding model. Anisotropic displacement parameters were used for all non-H atoms, while H-atoms were given isotropic displacement parameters equal to 1.2 (or 1.5 for methyl hydrogen atoms) times the equivalent isotropic displacement parameter for the atom to which the H-atom is attached. Refinement used SHELXL 96 [21]. Selected bond lengths and angles for the three complex cations may be found in Table I, while atomic coordinates for [Ni(**1**)(acac)][Ni(acac)$_3$]·THF, [Ni(**3**)(acac)][Ni(acac)$_3$]·THF and [Ni(**1**)$(OH_2)_2$]Cl_2 may be found in Tables II–IV, respectively.

Crystal Data for [Ni(1)(acac)][Ni(acac)$_3$]·THF

$C_{19}H_{33}N_2NiO_{4.5}$, M = 420.18, pale purple blocks, crystal dimensions 0.38 × 0.30 × 0.30 mm, monoclinic, space group P2(1)/n, **a** = 12.5245(2), **b** = 16.70720(10), **c** = 20.1930(3) Å, $\alpha = 90°$, $\gamma = 93.7680(10)°$, $\gamma = 90°$, **V** = 4216.24(10) Å^3 (by least squares refinement on 8192 reflection positions), Z = 8, T = 180(2)K, $D_{calc} = 1.324$ g/cm^3, Mo-Kα radiation (0.71073 Å), mu(MoKα) = 1.027 mm^{-1}, F(000) = 1800, Siemens SMART three-circle system with CCD area detector. Maximum θ was 28.63°, hkl ranges were −16/9, −21/21, −22/26. Goodness-of-fit on F^2 was 0.988, R1 = 0.0495 for 6088 reflections with $\mathbf{I} > 2\sigma(\mathbf{I})$, wR2 = 0.1199, 24880 measured reflections, 9857 unique reflections [R(int) = 0.0463], number of refined parameters 498, largest difference peak and hole 0.519 and −0.427 e -Å^{-3}.

Crystal Data for [Ni(3)(acac)][Ni(acac)$_3$]·THF

$C_{36}H_{62}N_4Ni_2O_9$, M = 812.32, pale purple blocks, crystal dimensions 0.4 × 0.2 × 0.1 mm, monoclinic, space group P2(1)/n, a = 12.4730(10), b = 15.9550(5), c = 20.308(2) Å, $\alpha = 90°$, $\beta = 95.283(5)°$, $\gamma = 90°$, V = 4024.3(5) Å^3 (by least squares refinement on 6416 reflection positions), Z = 4, T = 180(2)K, $D_{calc} = 1.341$ g/cm^3,

TABLE I Selected bond lengths (Å) and angles(°) for:

(i) Ni(**1**)(acac)$^+$			
Ni(1)–O(21)	2.017(2)	Ni(1)–N(8)	2.111(2)
Ni(1)–O(22)	2.018(2)	Ni(1)–N(11)	2.160(2)
Ni(1)–N(1)	2.107(2)	Ni(1)–N(4)	2.187(2)
O(21)–Ni(1)–O(22)	90.90(9)	N(1)–Ni(1)–N(11)	91.09(9)
O(21)–Ni(1)–N(1)	173.40(9)	N(8)–Ni(1)–N(11)	84.84(9)
O(22)–Ni(1)–N(1)	92.75(9)	O(21)–Ni(1)–N(4)	89.65(9)
O(21)–Ni(1)–N(8)	91.73(9)	O(22)–Ni(1)–N(4)	93.21(9)
O(22)–Ni(1)–N(8)	174.70(9)	N(1)–Ni(1)–N(4)	84.66(9)
N(1)–Ni(1)–N(8)	85.07(9)	N(8)–Ni(1)–N(4)	91.41(9)
O(21)–Ni(1)–N(11)	94.38(9)	N(11)–Ni(1)–N(4)	174.56(10)
O(22)–Ni(1)–N(11)	90.38(9)		
(ii) Ni(**3**)(acac)$^+$			
Ni(1)–O(23)	2.015(3)	Ni(1)–N(11)	2.063(3)
Ni(1)–O(26)	2.023(3)	Ni(1)–N(14)	2.142(3)
Ni(1)–N(17)	2.059(3)	Ni(1)–N(110)	2.149(3)
O(23)–Ni(1)–O(26)	89.93(12)	N(17)–Ni(1)–N(14)	84.90(13)
O(23)–Ni(1)–N(17)	177.11(12)	N(11)–Ni(1)–N(14)	82.18(13)
O(26)–Ni(1)–N(17)	92.64(12)	O(23)–Ni(1)–N(110)	96.85(12)
O(23)–Ni(1)–N(11)	91.96(13)	O(26)–Ni(1)–N(110)	95.03(12)
O(26)–Ni(1)–N(11)	178.05(13)	N(17)–Ni(1)–N(110)	81.61(13)
N(17)–Ni(1)–N(11)	85.46(13)	N(11)–Ni(1)–N(110)	84.29(13)
O(23)–Ni(1)–N(14)	96.06(12)	N(14)–Ni(1)–N(110)	161.58(13)
O(26)–Ni(1)–N(14)	98.08(12)		
(iii) Ni(**1**)$(OH_2)_2^{2+}$			
Ni(1)–O(1)	2.0909(13)	Ni(1)–O(2)	2.1071(12)
Ni(1)–N(8)	2.0921(13)	Ni(1)–N(4)	2.1509(14)
Ni(1)–N(1)	2.1035(13)	Ni(1)–N(11)	2.1581(13)
O(1)–Ni(1)–N(8)	94.68(5)	N(1)–Ni(1)–N(4)	85.24(6)
O(1)–Ni(1)–N(1)	172.18(6)	O(2)–Ni(1)–N(4)	96.32(5)
N(8)–Ni(1)–N(1)	86.16(5)	O(1)–Ni(1)–N(11)	96.81(5)
O(1)–Ni(1)–O(2)	84.36(5)	N(8)–Ni(1)–N(11)	85.56(5)
N(8)–Ni(1)–O(2)	172.05(5)	N(1)–Ni(1)–N(11)	91.01(5)
N(1)–Ni(1)–O(2)	95.87(5)	O(2)–Ni(1)–N(11)	86.71(5)
O(1)–Ni(1)–N(4)	86.97(5)	N(4)–Ni(1)–N(11)	175.39(5)
N(8)–Ni(1)–N(4)	91.51(5)		

TABLE II Comparison of *N—M—N* bond angles for several divalent metal ions with ligands **1** and **3** from crystal structures.[ref] Except where noted, all complexes are six coordinate $MLCl_2$

		Ligand **1**		Ligand **3**	
Metal ion	H.S. 6-coord. Ionic radius	$N_{ax}–M–N_{ax}$	$N_{eq}–M–N_{eq}$	$N_{ax}–M–N_{ax}$	$N_{eq}–M–N_{eq}$
Mn^{II}	97	158.0(2)	75.6(2)	144.0(2)	74.1(2)
Fe^{II}	92	161.88(5)	78.36(5)	145.78(7)	77.31(7)
Co^{II}	88.5	172.4(2)	81.11(13)	149.81(9)	80.86(8)
† CU^{II}	87	–	–	164.85(13)	83.92(14)
¶Ni^{II}	83	175.39(5)	86.16(5)	–	–
*Ni^{II}	83	174.56(10)	85.07(9)	161.58(13)	85.46(13)
†Cu^{II}	79	175.16(13)	85.30(12)	–	–

† Cu^{II} complex is $Cu(L)(MeCN)_2^{2+}$.
¶ Ni^{II} complex is $Ni(L)(OH_2)_2^{2+}$ (vide supra).
* Ni^{II} complexes are $Ni(L)(acac)^+$ (vide supra).
† Ionic Radius is for 5-coord Cu^{II}. Complex is $Cu(L)Cl^+$.

TABLE III Molar conductance of Ni^{II} chloride complexes in various solvents

Complex	Molar conductance			
	Water	Acetonitrile	DMF	Nitromethane
Ni(**1**)$Cl_2 \cdot 2H_2O$	185	127	61	32
Ni(**2**)$Cl_2 \cdot H_2O$	213	134	64	32
Ni(**3**)$Cl_2 \cdot 0.5H_2O$	205	176	62	21
[Ni(**4**)Cl]PF_6	171	123	70	80
1:1	118–131	120–160	65–90	75–95
2:1	235–273	220–300	130–170	150–180

Ref. [14] used for theoretical conductance values.

TABLE IV Redox potentials (*vs.* SHE) for the complexes with peak separations

Complex	E_{red} (V) Ni^{2+}/Ni^{+}	$E_{1/2}$ (V) Ni^{3+}/Ni^{2+}	$(E_a - E_c)$ (mV) Ni^{3+}/Ni^{2+}	E_{ox} (V)
Ni(**1**)$Cl_2 \cdot 2H_2O$	−1.894	+0.991	154	+1.325
Ni(**2**)$Cl_2 \cdot H_2O$	−1.991	+1.001	77	+1.323
Ni(**3**)$Cl_2 \cdot 0.5H_2O$	−2.036	+0.863	68	+1.450
[Ni(**4**)Cl]PF_6	−1.301	+1.760 (E_{ox})	106	+1.492

Mo-Kα radiation (0.71073 Å), mu(MoKα) = 1.027 mm^{-1}, F(000) = 1736, Siemens SMART three-circle system with CCD area detector. Maximum θ was 28.00°, hkl ranges were −16/14, −20/14, −25/27. Goodness-of-fit on F^2 was 1.010, R1 = 0.0544 for 4721 reflections with $I > 2\sigma(I)$, wR2 = 0.1350, 21463 measured reflections, 7883 unique reflections [R(int) = 0.0641], number of refined parameters 470, largest difference peak and hole 0.441 and −0.498 e -$Å^{-3}$.

Crystal Data for [Ni(1)$(H_2O)_2$]Cl_2

$C_{14}H_{34}N_4Ni_2Cl_2O_2$, M = 420.06, pale purple blocks, crystal dimensions 0.45 × 0.4 × 0.4 mm, orthorhombic, space group $P2_12_12_1$, a = 8.7765(2), b = 12.8899(2), c = 16.7200(3) Å, $\alpha = 90°$, $\beta = 90°$, $\gamma = 90°$, V = 1891.50(6) $Å^3$ (by least squares refinement on 8192 reflection positions), Z = 4, T = 180(2)K, D_{calc} = 1.475 g/cm^3, Mo-Kα radiation (0.71073 Å), mu(MoKα) = 1.322 mm^{-1}, F(000) = 896, Siemens SMART three-circle system with CCD area detector. Maximum θ was 28.55°, hkl ranges were −9/11, −16/17, −21/21. Goodness-of-fit on F^2 was 0.954, R1 = 0.0206 for 4132 reflections with $I > 2\sigma(I)$, wR2 = 0.0440, 11407 measured reflections, 4433 unique reflections [R(int) = 0.0212], number of refined parameters 227, largest difference peak and hole 0.379 and −0.322 e-$Å^{-3}$. For all structures, selected bond lengths and angles are in Table I.

RESULTS AND DISCUSSION

Ligand Solution Behavior

The literature [5,7] and our own prior studies informed us of the proton-sponge behavior of ethylene cross-bridged tetraazamacrocycles. In previous work [1], the potentiometric titration showed **1** to be a dibasic ligand with pK_{a1} = 9.58(3) and $pK_{a2} > 13$ (since the second proton was identified by stoichiometry but its deprotonation was not observed under normal aqueous conditions). In the present study, we have performed the potentiometric titrations of **2**–**4** to further quantitate their proton-sponge behavior.

Ligand **2** behaves similarly to **1** under aqueous conditions, exhibiting a single observable

deprotonation of $pK_{a2} = 6.71(2)$. However, the elemental analysis and the stoichiometry of the titration point to the presence of two additional protons whose pK_a's cannot be determined under normal aqueous conditions. Figure 2a shows the calculated and observed titration data for **2**. From this result, it is clear that the first proton dissociates with $pK_{a1} < 2$ and that the third proton dissociates with $pK_{a3} > 13$. Thus, in addition to having proton-sponge character, **2** is also able to bind a third proton, but very weakly.

Ligand **3** behaves as a tribasic ligand as well. Our experiments confirm the behavior initially reported by Bencini *et al.* [7], who synthesized the ligand by a different route and examined its solution behavior. This previous study found only $pK_{a2} = 5.95(1)$ and suggested $pK_{a1} < 1$, since deprotonation occurred below the observed pH region, and $pK_{a3} > 13$ since its deprotonation was not observed even at the maximum pH studied. Our own potentiometric titrations (Fig. 2b) confirm that the first deprotonation occurs below the pH region normally studied in aqueous solutions. However, we were able to observe both pK_{a2} and pK_{a3} under our conditions. According to our fit, $pK_{a2} = 5.77(2)$, which is similar to the value reported previously, but we find $pK_{a3} = 11.3(2)$ which does not agree well with the earlier study. The reliability of pK_{a3} is rather limited due to the high pH necessary for full deprotonation, but is nevertheless at a value observable in many other ligand titrations [22]. Fitting the titration curve without this second constant resulted in much higher GOF values.

The fact that all three deprotonations occur in a normal range indicates that ligand **3** is not a true proton sponge and that it behaves much more like an unbridged tetraazamacrocycle [22]. This difference from ligands **1** and **2** must arise from the smaller ring size of the 12-membered parent macrocycle, producing a shallower cavity which binds more protons than **1**, but binds them less strongly. The crystal structures [5, 8] of

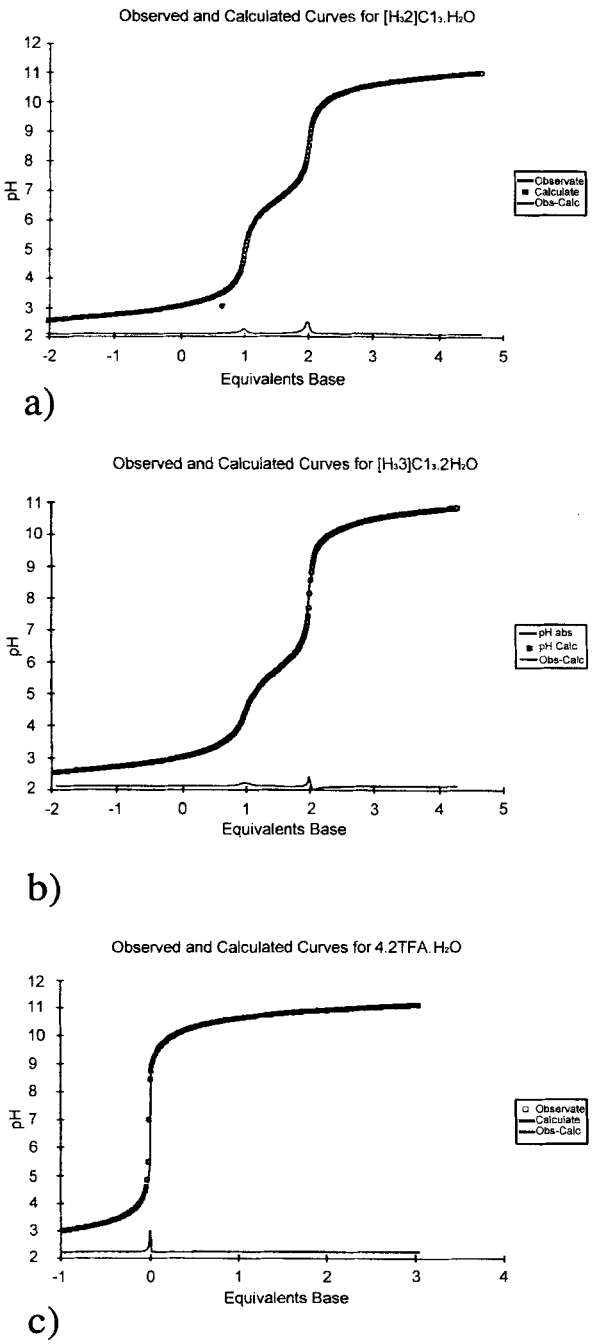

FIGURE 2 Titration data plotted against equivalents of base calculated per mole of (a) $2 \cdot 3HCl \cdot H_2O$ (b) $3 \cdot 3HCl \cdot 2H_2O$ and (c) $4 \cdot 2TFA \cdot H_2O$. The line through the data is the best fit of the data as found by BETA as described in the text. The line near the baseline is the residual (pH_{Obs}-pH_{Calc}) for this fit.

triprotonated **3** and diprotonated **1** and **4** identify the structural cause of this difference (Fig. 3). In diprotonated **1** and **4**, the two protonated methylated nitrogen atoms form strong hydrogen bonds to one bridgehead nitrogen each, giving six-membered H-bonded rings. In triprotonated **3**, both the protonated methylated nitrogens make no strong hydrogen bonds but one bridgehead nitrogen is protonated and forms a strong hydrogen bond to the other bridgehead nitrogen. Undoubtedly, this difference in hydrogen bonding pattern and in solution behavior arises from cavity size and flexibility. Although the crystal structure of triprotonated **2** has not yet been obtained, we can postulate that it has characteristics of both **1** and **3**. Because of the single trimethylene chain, a six-membered H-bonded ring can form; this is the probable site of the most strongly held proton responsible for the proton sponge character of **2**. The other half of the ligand, like **3**, contains only ethylene chains, and is probably the site of the other two, less strongly held protons.

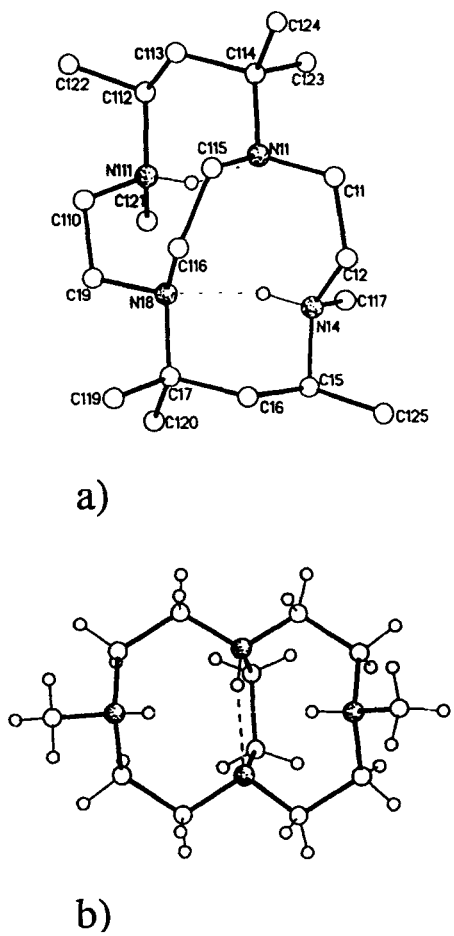

FIGURE 3 Crystal structures of (a) $4 \cdot 2TFA \cdot H_2O$ and (b) $3 \cdot 3HCl \cdot 2H_2O$ showing the difference in protonation position and hydrogen bonding.

The potentiometric titration of **4** reveals it to behave like **1** rather than like **3**. Ligand **4** is stoichiometrically diprotonated in aqueous solution, but like **1** and **2**, exhibits only one observable pK_a under normal aqueous conditions (Fig. 2c). Our experiment assigned $pK_{a1} = 11.45(3)$, which indicates the highest pH at which deprotonation has been observed for the four ligands studied. Again, pK_{a2} was not observed indicating that it is greater than 13 in water. The increase in basicity of **4** *vs.* **1** is possibly due to the increase in rigidity associated with the presence of 6 methyl substituents on carbon atoms of the ring. The six methyl substituents on the ring should enchance the immobilization of the nitrogen donors. Crystal structures [5,8] of diprotonated **1** and **4** (see Fig. 3a) show that their bicyclic skeletons have virtually identical conformations. Both ligands have their methylated nitrogen atoms protonated with strong hydrogen bonds to neighboring bridghead nitrogens, an energetically favorable arrangement apparently responsible for the exceptional proton affinities of these ligands.

Preparation of Metal Complexes

Quantitation of *the proton sponge problem* assured us that complexation would be most facile in non-protonic media. $Ni(acac)_2$ was chosen as a readily available anhydrous nickel(II) salt and initial complexation reactions with **1** and **3** were performed (Fig. 4a) in THF because of the good solubilities of both the ligands and the metal

a) $Ni(acac)_2 + L \xrightarrow{THF} [NiL(acac)][Ni(acac)_3]\,THF$

b) $NiCl_2 + L \xrightarrow[N_2]{DMF} NiLCl_2$ (L = **1-3**)

$NiCl_2 + L \xrightarrow[2.\ NH_4PF_6,\ MeOH]{1.\ DMF,\ N_2} [NiLCl]PF_6$ (L = **4**)

FIGURE 4 Preparation of Ni^{II} complexes of cross-bridged tetraazamacrocycles from (a) $Ni(acac)_2$ and (b) $NiCl_2$.

source in that solvent. The reactions were performed under an inert atmosphere, not to protect the metal from oxygen (as is normally the case) but to protect the ligand from moisture, and possibly oxygen, in the air. The unprotonated ligands are generally viscous colorless oils that yellow and become cloudy if stored in the air, but remain clear and colorless if stored under an inert atmosphere. While these initial reactions successfully produced the targeted complexes, two problems with this synthetic method were identified. First, the yield of the desired cation was rather low due to formation of salt of the complex anion $Ni(acac)_3^-$.The presence of the second Ni^{II} in the molecule also complicated the characterization of the new macrobicycle complexes since assignment of spectroscopic properties to a particular Ni^{II} type proved difficult.

To obtain a less complicated derivative, anhydrous $NiCl_2$ was reacted with ligands **1**–**4** in dry DMF under an inert atmosphere (Fig. 4b). This synthesis proved successful giving desired products in yields of between 69 and 89%. All further characterization employed the chloride complexes/salts.

Crystal Structures

While not ideal for some studies the acac complexes did prove easy to crystallize (by ether diffusion into THF solutions) and representations of the cations of $[Ni(\mathbf{1})(acac)^+]$ and $[Ni(\mathbf{3})(acac)^+]$ are shown in Figures 5a and 5b, along with that of the dication $Ni(\mathbf{1})(OH_2)_2^{2+}$ (Fig. 5c). These X-ray crystal structures confirm the expected geometric properties and provide insight into the solution behavior of the new compounds. As is the case for the structures [23] of ethylene cross-bridged complexes with the pseudo-octahedral metal ions Mn^{II},[1] Fe^{II}[1] and Co^{II}, (where the ligands are **1** and **3**), the ligands are constrained to have folded conformations by the short cross-bridge. In both cases, the macrobicycle occupies two axial and two *cis* equatorial sites of distorted octahedra, while the chelating acac ligand occupies the remaining *cis* equatorial sites. $Ni(acac)_3^-$ serves as the counter ion needed to balance the charge for both cationic complexes, and both of these structures include one THF molecule of crystallization. A second crystal structure of the N^{II} complex of **1** has been obtained from the $NiCl_2$ synthesis product (ether diffusion into an acetonitrile solution) and shows the ligand in a similar arrangement, but with two water molecules bound to the *cis* sites instead of the acac ligand. The diaqua dication's charge is balanced by two chloride anions that form a hydrogen bonding chain with the aquo ligands; one chloride bridges both water ligands of the same complex through hydrogen bonds, while the other bridges a single water ligand of two complexes intermolecularly.

These structures represent the first Ni^{II} complexes structurally characterized for ligands of this class. In the chemistry of the unbridged parent macrocycles, with few exceptions [24], 1,4,8,11-tetraazacycotetradecane, or *cyclam*, binds metal ions in a square planar fashion [25], occupying all four equatorial sites of octahedral complexes, which locates the two remaining ligand binding sites at the *trans*, axial positions. As stated earlier, [12]aneN4 is too small to fit completely around the metal ion, and generally folds to occupy two *cis* equatorial and the two axial sites on octahedral metal ions [26], a strict parallel to the coordination reported here

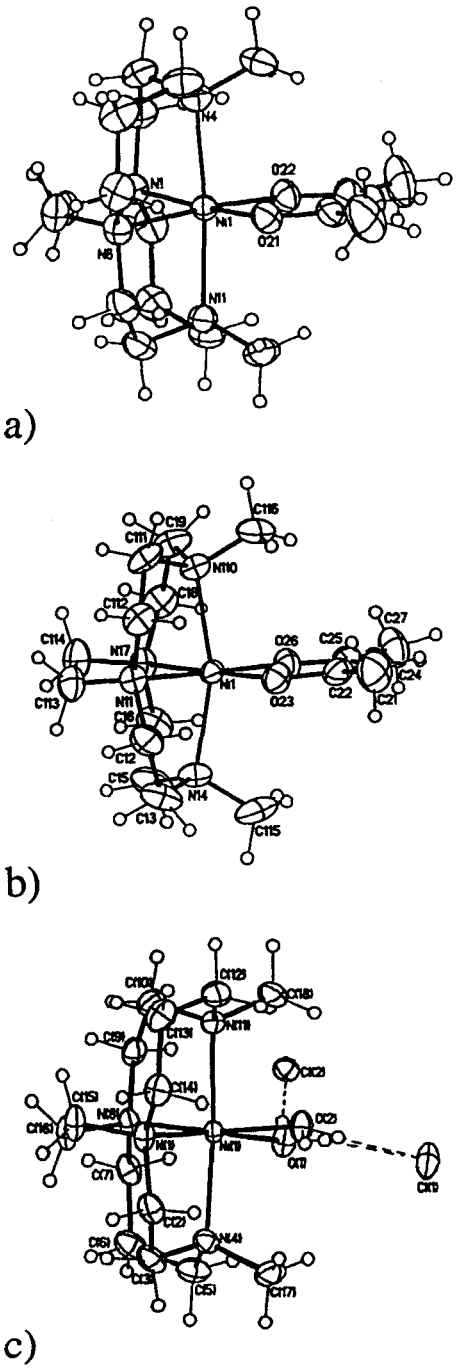

FIGURE 5 Views of the crystal structures of (a) Ni(**1**)(acac)$^+$ and Ni(**3**)(acac)$^+$ (c) Ni(**1**)$(OH_2)_2^{2+}$.

for **1** and **3**. The short cross-bridge of **1**, forces the [14]aneN4 ring system to behave more like [12]aneN4. The effects of the two *cis* labile sites on the reactivity of these complexes are currently being explored.

A more detailed inspection of the three structures shows that they follow several trends also present in the structures of the analogous Mn^{II}, Fe^{II} and Co^{II} complexes [1,23]. First, the size of the ring system dictates the distortion of the octahedra. The 14-membered ring in **1**, engulfs the metal ion more fully than does the 12-membered ring in **3**. The N_{ax}—M—N_{ax} bond angle for Ni(**1**)(acac)$^+$ is 174.56(10)1, and for Ni(**1**)$(OH_2)_2^{2+}$ it is 175.39(5)°, while for Ni(**3**)(acac)$^+$, it is only 161.58(13)1. This smaller angle for the smaller macrobicycle demonstrates how the metal ion fits less well into the ligand cavity.

A second general observation is that the smaller Ni^{2+} ion is more fully enfolded by both macrobicycles than the larger Mn^{2+}, Fe^{2+} and Co^{2+} ions but less so than Cu^{2+} [1,8,23]. Table II shows the smooth change in N_{ax}—M—N_{ax} bond angles as a function of the radius of the pseudo-octahedral ion. The presence of either a chelating acac ligand or two aqua ligands may influence these values since most of the structures are of $MLCl_2$ complexes. However, little deviation from the expected trend is observed except in the complex of ligand **3**, where the N_{eq}—Ni—N_{eq} angle is larger than expected, and in Ni(**1**)$(OH_2)_2^{2+}$ whose bond angles are larger than those of the related copper(II) complexes. The electron density of the hard oxygen donor and/or the steric bulk associated with the acac chelate may also influence the bond angles as compared to the larger, softer, monodentate chloride ligands present in the complexes of the other metal ions. The chloride ions probably take up more space than water molecules, allowing Ni^{2+} to sink more deeply into the cavity of the major ligand in the diaquo complex than would otherwise be expected. Although it is unclear

whether water or chloride is bound to nickel in the cases where water is included in the formula in the bulk solids, all the non-acac complexes will be described as chloro complexes for simplicity.

Finally, in these closely related structures, the mutual orientations of the N-methyl groups are important. In all cases the N-methyl groups project above and below the plane containing the nickel and the two labile ligands, an arrangement that may prevent dimerization by formation of M—O—M bridges (*vide infra*). For both structures of ligand **1**, the methyl groups are *gauche*, as viewed down the N_{ax}—M—N_{ax} *axis*, while in the complexes of **2**, the same view shows that the N-methyl groups are *eclipsed*. This phenomenon appears to be a result of the ligand size and symmetry and has been discussed elsewhere [1].

It is interesting that the rather bulky acac ligand has no steric difficulty binding to Ni^{2+} in these complexes. Recent studies with iron and manganese complexes of these same ligands demonstrate that the N-methyl groups prohibit dimerization [27], even under oxidizing conditions known to be favorable for formation of species of the types Fe—O—Fe and Mn—$(O)_2$—Mn [28]. Significantly, replacement of the methyl groups by H allows facile dimerization under mild oxidizing conditions for both the iron and manganese. The present structures reveal that steric prevention of dimerization must occur because dimerization would approximately superimpose the methyl groups from the two ligands. However, steric bulk in the plane orthogonal to the N_{ax}—M—N_{ax} plane, as in the acac examples, is not sterically precluded by the N-methyl groups. Discussions of in-plane *versus* out-of-plane steric bulk have appeared elsewhere [29].

Electronic Structure

The magnetic moments of the three complexes $NiLCl_2$ where L = **1**–**3** fall into a normal range for high spin, octahedral d^8 Ni^{II} complexes [13]. The values are: $\mu_{eff} = 3.09$ for Ni(**1**)Cl_2, $\mu_{eff} = 3.19$ for Ni(**2**)Cl_2 and $\mu_{eff} = 3.19$ for Ni(**3**)Cl_2. The magnetic moment of the Ni^{II} complex with ligand **4** was quite high however, $\mu_{eff} = 3.51$. This value is out of the range for a normal octahedral complex and led us to question the octahedral geometry, Ni(**4**)Cl_2, we had expected for the complex.

We had previously obtained [8] the crystal structures of [Cu(**4**)Cl]Cl and [Cu(**1**)Cl]Cl both of which are five-coordinate, but assumed this coordination number was determined by the metal ion and not related to the steric demands of the ligand, since our previous work on octahedral metal ions (with ligand **1**–**3**) clearly showed six-coordination to be possible. Yet, we did observe that Cu(**4**)Cl^+ was very nearly trigonal bipyramidal while Cu(**1**)Cl^+ and two previously published Cu^{2+} complexes of ethylene cross-bridged tetraazamacrocycles [6] are square pyramidal – seemingly the preferred geometry of Cu^{2+} with this donor set. While examining the *special* coordination geometry of Cu(**4**)Cl^+, we realized that the four methyl groups surrounding the labile binding site (two N-methyl groups and two of the geminal dimethyl groups) formed a shallow cavity which sterically prevented coordination of a second chloride ligand, or in the case of Cu^{2+}, adoption of a square pyramidal geometry [8] (Fig. 6). In Cache [7] molecular models, forcing a second chloride to bind or forcing the square pyramidal geometry shortened the distance between Cl and a methyl group to 2.4 Å, clearly an unfavorable distance. But in the trigonal bipyramidal structure, where the single Cl ligand is centered in the cavity, this distance was no less than 3.0 Å [8]. A subsequent determination of the crystal structure of Co(**4**)Cl^+ [23] show that it adopts the same five-coordinate geometry even though Co(**1**)Cl_2 and Co(**2**)Cl_2 are six-coordinate and octahedral, confirming our belief that the ligand **4** generally limits complexes to five-coordination. These results, along with the high value of

FIGURE 6 A space filling diagram of Cu(**4**)Cl^+ showing the shallow cavity defined by ligand methyl groups filled by a single chloride ligand.

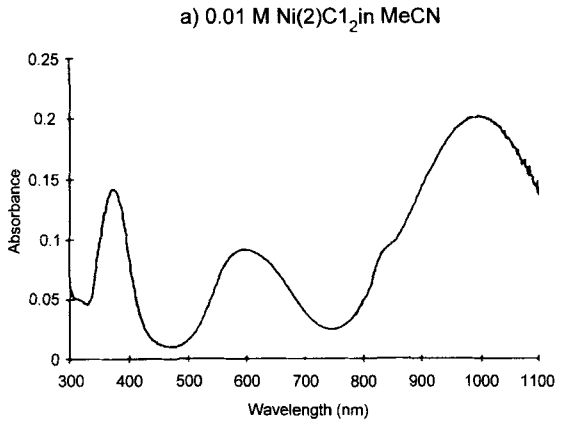

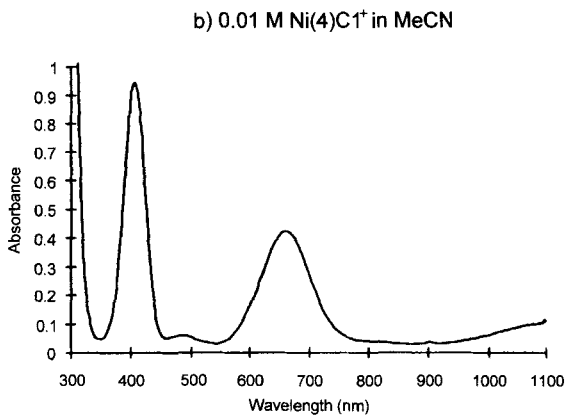

FIGURE 7 Electronic spectra of (a) Ni(**2**)Cl_2 and (b) [Ni(**1**)Cl]PF_6 in acetonitrile.

μ_{eff} for the Ni^{2+} complex of **4**, a known property of five-coordinate Ni^{2+} [30], convince us that the complex should be formulated as [Ni(**4**)Cl]PF_6.

The electronic spectra of the four chloride complexes reinforce our conclusions about the coordination geometries. $NiLCl_2$ (L = **1**–**3**) all exhibit classic octahedral Ni^{2+} electronic spectra, with three major absorptions in the range of 300–1100 nm, as exemplified by the spectrum of Ni(**2**)Cl_2 in acetonitrile (Fig. 7a). However, [Ni(**4**)Cl]PF_6 displays a very different spectrum that is consistent with five-coordination [30b, 31]. Literature examples of trigonal bipyramidal Ni^{2+} complexes with N_4Cl donor sets most closely resemble that of [Ni(**4**)Cl]PF_6. These complexes have only two major absorptions in the 300–1100 nm range, with extinction coefficients larger than normal for octahedral Ni^{2+}. One band is usually centered at about 700–800 nm with an extinction coefficient approximately twice that of the other, which is centered at about 400–500 nm [30b, 31]. Calculations using the crystal field model agree with the assignment of these observed electron spectra to high spin Ni^{II} in a trigonal bipyramidal ligand field [32]. Clearly, the spectrum of Ni(**4**)Cl^+ better approximates those of known examples of this geometry than classic octahedral spectra of $NiLCl_2$ (L = **1**–**3**).

The electronic spectra of octahedral Ni^{2+} complexes are particularly useful for determination of the the ligand field strengths of ligands [33]. Δ_o is directly given by the energy of the lowest energy absorption band. For the three octahedral dichloro complexes this gives the following results: $\Delta_o = 10{,}215\,cm^{-1}$ for Ni(**1**)Cl_2, $\Delta_o = 10{,}060\,cm^{-1}$ for Ni(**2**)Cl_2 and $\Delta_o = 9{,}843\,cm^{-1}$ for Ni(**3**)Cl_2. Clearly, the larger macrobicycle the larger its ligand field strength for Ni^{2+}. Probably, it forms a less distorted octahedron as noted above in the N_{ax}—M—N_{ax}

bond angles of the Ni(**1**)(acac)$^+$ and Ni(**3**)(acac)$^+$ crystal structures. Comparisons of these values with those of Ni^{2+} complexes with some unbridged tetraazamacrocycles is enlightening. The value [34] for *cis*-Ni(13[ane]N4)Cl_2 is $\Delta_o = 11{,}111\,cm^{-1}$ while that for *cis*-Ni(TACD)$(NO_3)_2$ is $\Delta_o = 9{,}756\,cm^{-1}$ (TACD = 1,4,7,10-tetrabenzyl-1,4,7,10-tetraazacyclododecane) [30b]. Thus the ligand field strengths of our ethylene cross-bridged tetraazamacrocycles are very similar to those of unbridged analogues which bind in a similar *cis* fashion. The value Dq_{xy} is the measure of ligand field strength analogous to Δ_o for tetragonally distorted complexes [35], the usual geometry of tetraazamacrocycles that chelate in a planar fashion. Values for Dq_{xy} are consistently much higher than those of Δ_o for *cis*-binding of analogous ligands and this is also true of our ethylene cross-bridged ligands. For example $Dq_{xy} = 14{,}870\,cm^{-1}$ for *trans*-Ni(14[ane]N4)Cl_2 [35], which is much higher than Δ_o of Ni(**1**)Cl_2 given above. In the case of our cross-bridged ligands, planar coordination is topologically prevented, producing high spin Ni^{2+} complexes of the typical lower ligand field strengths associated with *cis*-tetraazamacrocycles.

Solution Properties

The results of conductance experiments on the chloride complexes (Tab. III) reflect the ease with which the chloride ligands may be replaced by solvent. The ionization (displacement of chloride by solvent) of these complexes in solution correlates with the dielectric constant and coordinating ability of the solvent. In the low dielectric, non-coordinating solvent, nitromethane, the six-coordinate complexes approach the behavior of non-electrolytes, revealing that the chlorides remain bound and indicating that the structure of the complex in solution is probably six-coordinate and pseudo octahedral, as in the solid state. In contrast, the five-coordinate complex [Ni(**4**)Cl]PF_6 behaves, as expected, as a 1:1 electrolyte but without dissociation of the one bound chloride ligand. In coordinating solvents with slightly higher dielectric constants, like acetonitrile and DMF, all four complexes behave as 1:1 electrolytes which implies that solvent has displaced one chloride ligand from the coordination sphere of the six-coordinate complexes. In water, behavior intermediate between a 1:1 and 2:1 electrolyte is observed for all of the complexes, indicating that the last chloride ligand has only been partially replaced by water molecules in both the five and six-coordinate complexes. For solid samples where water is present in the composition, it has not been definitively determined whether water or chloride is bound to the nickel. Thus, in some cases the conductivity behaviour may reflect chloride replacing water, rather than solvent replacing chloride.

Electrochemical Studies

The cyclic voltammograms of (a) [Ni(**4**)Cl]PF_6 and (b) Ni(**3**)Cl_2, in MeCN are shown in Figure 8. The latter, **8b**, is representative of the six-coordinate chloro complexes. The redox potentials and peak separations of all four chloro complexes can be found in Table IV. These rigid ligands stabilize a range of oxidation states for nickel, from Ni^+ to Ni^{3+} as shown by the reversible oxidation, assigned as the $Ni^{2+/3+}$

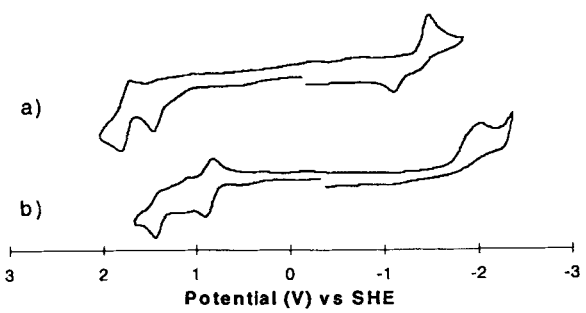

FIGURE 8 Cyclic voltammograms of (a) [Ni(**4**)Cl]PF_6 and (b) Ni(**3**)Cl_2 in acetonitrile. Complexes were 0.001 M in acetonitrile made 0.1 M in tetrabutylammonium hexafluorophosphate.

cycle, and irreversible reduction, to Ni^+, for $NiLCl_2$ (L = **1**–**3**) and [Ni(**4**)Cl]PF_6. Also of note is the ring size effect from the 14-membered **1** through the 12-membered **3**. The smallest ring complex (L = **3**) is much easier to oxidize, which may be explained simply on the basis of metal ion size; the smaller cavity more greatly stabilizes the smaller oxidized metal ion. Conversely, the larger ligands favor the larger, lower valent metal ion which is demonstrated in the easier reduction of the complexes of the larger macrobicyclic ligands. The more difficultly oxidized complexes of **1** contain a metal ion more completely enclosed by the macrobicyclic cavity and more removed from the solvent, as shown in the N_{ax}—M—N_{ax} and N_{eq}—M—N_{eq} bond angles (*vide supra*).

The presence of a second, irreversible oxidation for all four complexes is clear, but its origin has not been assigned. The sequence of the reversible $Ni^{2+/3+}$ wave followed by the second irreversible oxidation is the same for all three octahedral complexes, while this order is reversed in the voltammogram of [Ni(**4**)Cl]PF_6. The probable source of the second oxidation process is the irreversible oxidation of bound chloride ligand. Since its potential depends on the complex, it is unlikely to involve free chloride.

The striking features of the voltammogram for [Ni(**4**)Cl]PF_6 are its much higher potential for the $Ni^{2+/3+}$ couple and the much milder potential for its irreversible reduction to Ni^+ compared to the three six-coordinate complexes. The much milder reduction of [Ni(**4**)Cl]PF_6 is probably due to the preference of Ni^+, a d^9 ion, for five coordination. This reduction is the only one exhibiting a return oxidation, although it is displaced by some 380 mV. We surmise that loss of Cl^- by the reduced Ni^+ accounts for the lack of reversibility here and in the other complexes. [Ni(**4**)Cl]PF_6 must be more difficult to oxidize as a result of its unique geometry as well. Ni^{3+} is apparently less well stabilized by the five-coordinate trigonal bipyramidal geometry than by the pseudo-octahedral geometries allowed by the other ligands.

Acknowledgments

The funding of this research by the Procter and Gamble Company is gratefully acknowledged. T. J. H. thanks the Madison and Lila Self Graduate Research Fellowship of the University of Kansas for financial support. We thank EPSRC and Siemens Analytical Instruments for grants in support of the diffractometer. The Kansas/Warwick collaboration has been supported by NATO.

Supporting Information Available: Tables of atomic coordinates and equivalent isotropic parameters, bond distances and angles, anisotropic displacement parameters, hydrogen coordinates and isotropic displacement parameters for [Ni(**1**)(acac)][Ni(acac)$_3$]·THF, [Ni(**3**)(acac)][Ni(acac)$_3$]·THF and [Ni(**1**)(OH$_2$)$_2$]Cl$_2$ (21 pages). Ordering information is given on any current masthead page.

References

[1] Hubin, T. J., Buchalova, M., McCormick, J. M., Collinson, S. R., Perkins, C. M., Alcock, N. W., Kahol, P. K., Raghunathan, A. and Busch, D. H. (2000). *J. Am. Chem. Soc.*, **122**, 2512.

[2] Busch, D. H. (1993). *Chem. Rev.*, **93**, 847.

[3] (a) Alexander, M. D. and Busch, D. H. (1966). *J. Am. Chem. Soc.*, **88**, 1130; (b) Chin, J., Banaszczyk, M., Jubian, V. and Zou, X. (1989). *J. Am. Chem. Soc.*, **111**, 186; (c) Hettich, R. and Schneider , H.-J. (1997). *J. Am. Chem. Soc.*, **119**, 5638; (d) Arciero, D. M. and Lipscomb, J. D. (1986). *J. Biol. Chem.*, **261**, 2170; (e) Halfen, J. A., Mahapatra, S., Wilkinson, E. C., Kaderli, S., Young, V. G. Jr., Que, L. Jr., Zuberbühler, A. D. and Tolman, W. B. (1996). *Science*, **271**, 1397; (f) Ross, P. K. and Solomon, E. I. (1991). *J. Am. Chem. Soc.*, **113**, 3246.

[4] (a) Cabiness, D. K. and Margerum , D. W. (1970). *J. Am. Chem. Soc.*, **92**, 2151; (b) Lindoy, L. F. (1986). *The Chemistry of Macrocyclic Ligand Complexes*, Cambridge University Press: Cambridge, p. 186.

[5] Weisman, G. R., Rogers, M. E., Wong, E. H., Jasinski, J. P. and Paight, E. S. (1990). *J. Am. Chem. Soc.*, **112**, 8604.

[6] Weisman, G. R., Wong, E. H., Hill, D. C., Rogers, M. E., Reed, D. P. and Calabrese, J. C. (1996). *J. Chem. Soc., Chem. Commun.*, p. 947.

[7] Bencini, A., Bianchi, A., Bazzicalupi, C., Ciampolini, M., Fusi, V., Micheloni, M., Nardi, N., Paoli, P. and Valtancoli, B. (1994). *Supramol. Chem.*, **3**, 41.

[8] Hubin, T. J., McCormick, J. M., Alcock, N. W. and Busch, D. H. (1999). *J. Am. Chem. Soc.*, submitted.
[9] Irving, H. and Williams, R. J. P. (1953). *J. Chem. Soc.*, **part III**, 3192.
[10] (a) Hubin, T. J., McCormick, J. M., Collinson, S. R., Alcock, N. W. and Busch , D. H. (1998). *J. Chem. Soc., Chem. Commun.*, p. 1675; (b) Busch, D. H., Collinson, S. R. and Hubin, T. J., *Catalysts and Methods for Catalytic Oxidation*, WO 98/39098, Sept. 11, 1998; (c) Busch, D. H., Collinson, S. R., Hubin, T. J., Labeque, R., Williams, B. K., Johnston, J. P., Kitko, D. J., Burkett-St. Laurent, J. C. T. R. and Perkins, C. M., Bleach Compositions, WO 98/39406, Sept. 11, 1998.
[11] Barefield, E. K., Wagner, F., Herlinger, A. W. and Dahl, A. R. (1976). *Inorg. Synth.*, **16**, 220.
[12] Perrin, D. D., Armarego, W. L. F. and Perrin, D. R. (1980). *Purification of Laboratory Chemicals*, 2nd edn., Pergamon Press: New York.
[13] *Inorganic Chemistry: Principles of Structure and Reactivity* (1993). 4th edn. Huheey, J. E., Keiter, E. A. and Keiter, R. L., Harper Collins, New York, p. 463.
[14] (a) Angelici, R. J. (1986). *Synthesis and Techniques in Inorganic Chemistry*, University Science Books: Mill Valley, CA; Appendix 2; (b) Feltham, R. D. and Hayter, R. G. (1964). *J. Chem. Soc.*, p. 4587; (c) Geary, W. J. (1971). *Coord. Chem. Rev.*, **7**, 81.
[15] Turowski, P. N., Rodgers, S. J., Scarrow, R. C. and Raymond, K. N. (1988). *Inorg. Chem.*, **27**, 474.
[16] McCormick, J. M. and Raymond, K. N., unpublished results.
[17] (a) Avdeef, A. and Raymond, K. N. (1979). *Inorg. Chem.*, **18**, 1605; (b) Harris, W. R. and Raymond , K. N. (1979). *J. Am. Chem. Soc.*, **101**, 6534.
[18] SMART User's manual, Siemens Industrial Automation Inc, Madison, Wis. USA.
[19] Cosier, J. and Glazer, A. M. (1986). *J. Appl. Cryst.*, **19**, 105.
[20] Sheldrick, G. M. (1990). *Acta Cryst.*, **A46**, 467.
[21] Sheldrick, G. M. (1996). SHELX-96 (beta-test) (including SHELXS and SHELXL), University of Göttingen.
[22] Martell, A. E., Smith, R. M. and Motekaitis, R. J. (1995). *NIST Standard Reference Database 46, Version 2.0*; NIST Standard Reference Data: Gaithersberg, MD.
[23] Hubin, T. J., McCormick, J. M., Alcock, N. W., Clase, H. J. and Busch, D. H. (1999). *Inorg. Chem.*, **38**, 4435.
[24] (a) Brewer, K. J., Calvin, M., Lumpkin, R. S., Otvos, J. W. and Spreer, L. O. (1989). *Inorg. Chem.*, **28**, 4446; (b) Che, C.-M., Kwong, S.-S., Poon, C.-K., Lai, T.-F. and Mak, T. C. W. (1985). *Inorg. Chem.*, **24**, 1359; (c) Poon, C.-K. and Che, C.-M. (1981). *J. Chem. Soc., Dalton Trans.*, p. 1336; (d) Lai, T.-F. and Poon, C.-K. (1976). *Inorg. Chem.*, **15**, 1562.
[25] (a) Fabbrizzi, L. (1985). *Comments Inorg. Chem.*, **4**(1), 33; (b) Martin, L. Y., Sperati, C. R. and Busch, D. H. (1977). *J. Am. Chem. Soc.*, **99**, 2968; (c) Martin, L. Y., Zompa, L. J., DeHayes, L. J. and Busch , D. H. (1974). *J. Am. Chem. Soc.*, **96**, 4046.
[26] (a) Henrick, K., Tasker, P. A. and Lindoy, L. F. (1985). *Progess Inorg. Chem.*, **33**, 1; (b) Busch, D. H. (1978). *Accts. Chem. Res.*, **11**, 392; (c) Iitaka, Y. S., Shina, M. and Kimura, E. (1974). *Inorg. Chem.*, **13**, 2886; (d) Collman, J. P. and Schneider, P. W. (1966). *Inorg. Chem.*, **5**, 1380.
[27] Hubin, T. J., McCormick, J. M., Alcock, N. W., Clase, H. J. and Busch, D. H. (1999). In preparation.
[28] (a) Lippard, S. J. (1988). *Angew. Chem. Int. Ed., Engl.*, **27**, 344; (b) Law, N. A., Caudle, M. T. and Pecoraro, V. L., In: *Advances in Inorganic Chemistry*, Vol. 46, Sykes, A. G., Ed., Academic Press, San Diego, 1999, p. 305.
[29] Huynh, M. H., Jameson, D. L., Churchill, M. R. and Takeuchi, K. 216th American Chemical Society Meeting, Boston, MA, August 23–27, Inorganic Division, paper 364.
[30] (a) Ciampolini, M. and Speroni, G. P. (1966). *Inorg. Chem.*, **5**, 45–49; (b) Kalligeros, G. A. and Blinn, E. L. (1972). *Inorg. Chem.*, **11**, 1145; (c) Goedken, V. L., Quagliano, J. V. and Vallarino, L. M. (1969). *Inorg. Chem.*, **11**, 2331.
[31] Ciampolini, M. and Nardi, N. (1966). *Inorg. Chem.*, **5**, 41–44.
[32] Ciampolini, M. (1966). *Inorg. Chem.*, **5**, 35–40.
[33] *Physical Methods for Chemists*, 2nd edn., Drago, R. S., Saunders College Publishing-Harcourt Brace Jovanovich, Ft. Worth, 1992. p. 438.
[34] Martin, L. Y., *Ph.D. Thesis*, The Ohio State University, 1974.
[35] Martin, L. Y., Sperati, C. R. and Busch, D. H. (1977). *J. Am. Chem. Soc.*, **99**, 2968.